

An Enabling Trajectory Planning Scheme for Lane Change Collision Avoidance on Highways

Zhiqiang Zhang^{ID}, Lei Zhang^{ID}, Member, IEEE, Junjun Deng^{ID}, Mingqiang Wang^{ID}, Zhenpo Wang^{ID}, Member, IEEE, and Dongpu Cao^{ID}, Member, IEEE

Abstract—This paper presents a hierarchical three-layer trajectory planning framework to realize real-time collision avoidance under complex driving conditions. This is mainly ascribed to the generation of a collision-free trajectory cluster based on the speed and the path re-planning. The upper-layer controller is to generate a reference quintic polynomial trajectory based on the Sequential Quadratic Programming by assuming mild speed and acceleration variations of the surrounding vehicles. The waypoints and time stamps can be obtained via the reference trajectory. When the assumption is invalid under complex driving conditions, the middle-layer controller would generate a Quadratic Programming-based trajectory cluster to assign different time stamps to each waypoint through time-based sampling methods. The lower-layer controller would be triggered to create a new feasible trajectory based on the path sampling if the collision avoidance requirements are not satisfied. The host vehicle will return to its original lane if no feasible time window is available to perform a lane change maneuver under the vehicle kinematics and lane change time/displacement constraints. The effectiveness of the proposed scheme is verified under various scenarios through comprehensive simulations.

Index Terms—Collision avoidance, trajectory planning, speed re-planning, path re-planning.

I. INTRODUCTION

AUTONOMOUS vehicles (AVs) exhibit enormous potential for increasing road capacity, promoting transport safety and reducing fuel consumption [1]–[3]. Lane change is a typical and nontrivial maneuver. Inappropriate lane change maneuvers are a major cause of road accidents in highway driving environments [4], [5]. Recently, the development of Vehicle-to-Vehicle (V2V) and Vehicle-to-Infrastructure (V2I) communication technologies enables the real-time acquisition of the information of all traffic participants in vicinity [6]. This can facilitate safe and feasible lane change maneuvers.

Manuscript received 18 February 2021; revised 17 May 2021 and 25 August 2021; accepted 18 September 2021. Date of publication 6 October 2021; date of current version 23 January 2023. This work was supported in part by Beijing Municipal Science and Technology Commission via the Beijing Nova Program under Grant Z201100006820007 and in part by the Ministry of Science and Technology of the People's Republic of China under Grant 2017YFB0103600. (Corresponding author: Lei Zhang.)

Zhiqiang Zhang, Lei Zhang, Junjun Deng, Mingqiang Wang, and Zhenpo Wang are with the Collaborative Innovation Center for Electric Vehicles in Beijing and the National Engineering Laboratory for Electric Vehicles, Beijing Institute of Technology, Beijing 100081, China (e-mail: 3120205211@bit.edu.cn; lei_zhang@bit.edu.cn).

Dongpu Cao is with the Mechanical and Mechatronics Engineering, University of Waterloo, Waterloo, ON, N2L 3G1, Canada.

Color versions of one or more figures in this article are available at <https://doi.org/10.1109/TIV.2021.3117840>.

Digital Object Identifier 10.1109/TIV.2021.3117840

Decision making [7], trajectory planning [8] and motion control [9] constitute a complete control loop for automated lane change maneuvers [10], [11]. Trajectory planning is responsible for generating collision-free and feasible trajectories [12]–[14]. The existing trajectory planning approaches for lane change can be assorted into three groups, i.e., function-based [5], [15], [16], search and grid-based [17], [18] and model-based methods [10], [14], [19]. Typical function-based curves include polynomial [15], [16], sinusoid [20], [21], B-Spline [22], [23] and Bezier curves [13]. Recent studies have compared these curves for trajectory planning and the quintic polynomial stands out due to its smooth acceleration and jerk profiles [24]. Search and grid-based methods have high computational intensiveness as they require sampling the whole space. Similarly, high modelling complexity inherent with model-based methods hinders their feasibility for real-time implementation [10], [25]. The mentioned methods focus on generating a continuous path rather than a trajectory without considering real-time collision avoidance.

The studies on collision avoidance during the lane change process are insufficient. Luo *et al.* proposed a Dynamic Lane Change Trajectory Planning (DLTP) model using the quintic polynomial based on V2V communication [26]. However, the target longitudinal vehicle speed was considered constant in deriving the lane change trajectory, which contradicted practical conditions and reduced the availability of feasible solutions. To tackle this issue, Yang *et al.* developed a DLTP model to determine the starting point for lane change maneuver [27]. However, only sampling the longitudinal vehicle displacement will result in frequent switchings of trajectory destinations. Peng *et al.* addressed a lane change trajectory model by formulating vehicle lateral acceleration using a Gauss distribution function [21]. However, the proposed method assumed constant accelerations of the surrounding vehicles, which significantly curtails its efficacy in handling emergency scenarios with abrupt accelerations [13]. Zhou *et al.* determined an optimal lane change trajectory using the TOPSIS algorithm in a collision-free trajectory cluster, in which the cubic polynomial lane change curve was converted into a function with one tuning parameter by assuming an unchanged longitudinal vehicle velocity [16]. Nevertheless, the assumption is difficult to hold in real-world driving conditions. Besides, the cubic vehicle speed profile of the host vehicle has only one extreme point, which can hardly describe its speed changing process.

The existing studies have invariably used longitudinal displacement sampling to realize collision-free lane change. This may result in frequent switchings of vehicle attitude and trajectory destination. Obstacle avoidance through re-planning

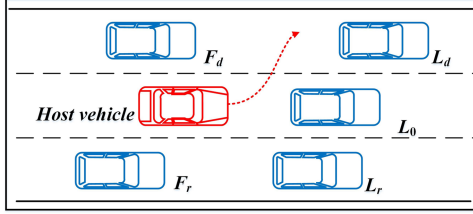


Fig. 1. A typical lane change scenario.

time-related speeds and accelerations may avail under such circumstances. A typical lane change scenario with five vehicles is illustrated in Fig. 1. When L_d executes a sudden deceleration during the lane change process of the host vehicle, it is feasible to avoid collision through re-planning the speeds and accelerations at each waypoint while achieving the same destination.

To address the mentioned issues as well as to distinguish with the existing studies, the major contributions of this study can be summarized as follows. First, a hierarchical scheme consisting of a reference trajectory and a collision-free trajectory cluster generation module is proposed. It allows for collision-free lane change options even when the motion states of the surrounding vehicles change abruptly. Second, a time-sampling-based speed re-planning is introduced to avoid potential collisions while maintaining vehicle attitude and destination and achieving high computational efficiency. Third, the relationship and trigger conditions between the speed and the path re-planning are given to meet the requirements of collision avoidance in different driving scenarios.

The remainder of this paper is structured as follows. Section II elaborates on the system architecture and the reference quintic polynomial trajectory generation module. Section III presents the speed re-planning method. Section IV explains the path re-planning method. Section V provides simulation verifications under various scenarios, followed by the key conclusions summarized in Section VI.

II. REFERENCE TRAJECTORY GENERATION

Trajectory planning is responsible for generating a drivable and collision-free trajectory from the current position to a destination. To realize real-time collision avoidance, it is vital to predict the motions of the surrounding vehicles and to detect the potential collision risks especially in dynamic and complex highway driving environments.

A. System Architecture

This study presents a hierarchical three-layer planner for collision-free lane change trajectory generation as shown in Fig. 2. A lane change decision needs to be determined by the decision-making module before executing a lane change maneuver [28], [29]. Once the lane change safety requirements are fulfilled, the hierarchical trajectory planning scheme will be executed.

The proposed lane change trajectory planning scheme includes the generations of a lane change reference trajectory based on the SQP and two collision-free trajectory clusters based on the speed and the path re-planning using the QP. The reference trajectory is generated based on the quintic polynomial

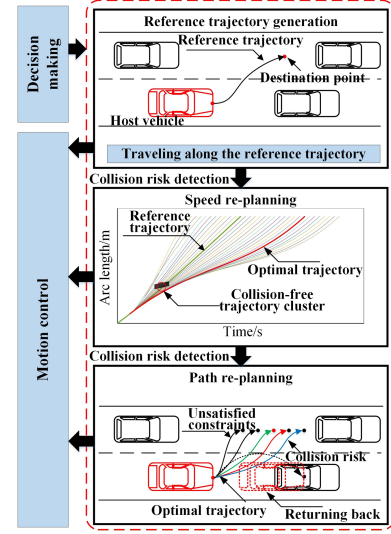


Fig. 2. The overall architecture of the proposed lane change trajectory planning scheme.

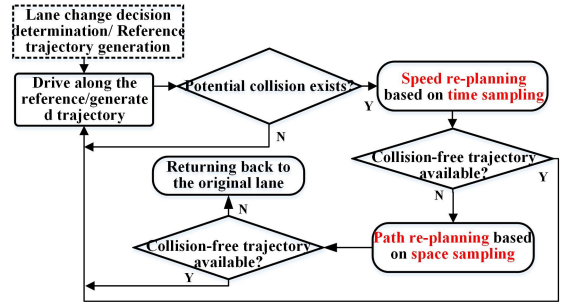


Fig. 3. The logic diagram of the proposed lane change trajectory planning scheme.

within road boundaries and vehicle kinematics constraints by assuming constant motion states of the surrounding vehicles. The host vehicle will drive along the reference trajectory until a potential collision is detected due to the unexpected motion state changes of the surrounding vehicles. In this case, the speed re-planning module will be triggered and the host vehicle would first attempt to avoid the potential collision via speed re-planning. Specifically, a series of time stamps can be sampled at a specific time step to determine the time of arrival at the same destination. Through incorporating the boundary constraints into a constrained optimization problem formulation, a collision-free trajectory cluster can be obtained. To select an optimal collision-free trajectory, the motions of the surrounding vehicles are depicted in the Space-Time (ST) graph. If it fails to find a feasible solution under the constraints in the speed re-planning, the destination will be sampled at specific arc length steps and a collision-free trajectory cluster with different longitudinal displacements will be generated. Then the optimal lane change trajectory can be determined based on a cost function considering acceleration, jerk and transport efficiency. Finally, the host vehicle will return to its origin lane if there is potential collision that cannot be avoided by the described re-planning scheme.

The logic diagram of the proposed hierarchical trajectory planning scheme is depicted in Fig. 3.

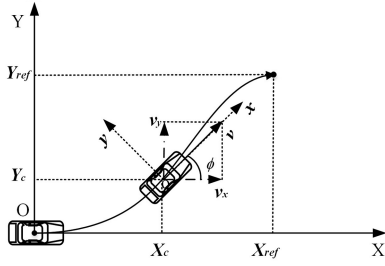


Fig. 4. The fixed earth and the local vehicle coordinate system.

Remark 1: Trigger signals are designed for each module. Only when the current trajectory fails to satisfy the safety requirements will the next module be triggered. The transitions between each module are described and only one module is active at any time during the entire lane change process.

Remark 2: The collision avoidance algorithm is developed by assuming known lane change of the host vehicle and motions of the surrounding vehicles. Related studies can be found in [28]–[32].

B. Feasible Reference Trajectory Generation via SQP

The two coordinate systems, i.e., the fixed earth XOY and the local vehicle xoy coordinate system, are introduced in Fig. 4. The vehicle configuration is represented as a vector $\mathbf{U} = [X_c, Y_c, \phi]$ in the fixed earth coordinate system, where (X_c, Y_c) is the vehicle's location and ϕ is the angle between the X -axis and the vehicle's instantaneous motion. The longitudinal and lateral vehicle velocities in the XOY coordinate system can be calculated by $v_x = v \cdot \cos\phi$ and $v_y = v \cdot \sin\phi$, where v is the vehicle velocity in the XOY coordinate system while it represents the longitudinal vehicle velocity in the xoy coordinate. Moreover, the ‘Point Mass Model’ is adopted to represent the host vehicle during the lane change process, and the heading of the vehicle is assumed to be aligned with its actual moving direction. Hence, the lateral vehicle velocity in the xoy coordinate and the vehicle sideslip angle are equal to zero.

The reference trajectory generation module will be triggered once receiving the enabling signal from the decision-making module. The continuity of the third derivative of the trajectory and a smooth curvature must be guaranteed to satisfy vehicle actuator characteristics. The quintic polynomial is used in this study, which is given by

$$\begin{cases} x = x(t) = \sum_{i=0}^5 p_i * t^i \\ y = y(t) = \sum_{j=0}^5 q_j * t^j \end{cases} \quad (1)$$

where x and y are the longitudinal and lateral displacements of the host vehicle at time step t ; p_i and q_j are the coefficients determining the trajectory shape. Since the longitudinal and lateral displacements are expressed using time-based functions, the velocities v_x and v_y and the accelerations a_x and a_y at each timestamp can be easily obtained by taking the first and second derivatives. The boundary conditions are given by

$$\begin{cases} x(0) = x_0, \dot{x}(0) = v_{x0}, \ddot{x}(0) = a_{x0} \\ y(0) = y_0, \dot{y}(0) = v_{y0}, \ddot{y}(0) = a_{y0} \end{cases} \quad (2)$$

$$\begin{cases} x(t_{lc}) = x_{lc}, \dot{x}(t_{lc}) = v_{xlc}, \ddot{x}(t_{lc}) = a_{xlc} \\ y(t_{lc}) = y_{lc}, \dot{y}(t_{lc}) = v_{ylc}, \ddot{y}(t_{lc}) = a_{ylc} \end{cases} \quad (3)$$

where $x_0, y_0, v_{x0}, v_{y0}, a_{x0}$, and a_{y0} are the longitudinal and lateral coordinate positions, velocities, and accelerations at the initial time step of the lane changing process, and $x_{lc}, y_{lc}, v_{xlc}, v_{ylc}, a_{xlc}, a_{ylc}$ at the final time step, respectively. Here, the initial position of the host vehicle is assumed to be specified at $(0, 0)$; the final lateral displacement is assumed to be the lane width of 3.75 m; the lateral velocity v_{ylc} and the longitudinal and lateral accelerations a_{xlc} and a_{ylc} are all assumed to be null. However, the lane change time t_{lc} and the longitudinal displacement x_{lc} are highly relevant to incumbent traffic conditions. It is worth mentioning that the longitudinal velocity of the host vehicle at the final time step v_{xlc} should be between the longitudinal velocities of the vehicles on the adjacent lane to avoid collision. This is given by

$$v_{xlc} \in (\min(v_{x_Fd}, v_{x_Ld}), \max(v_{x_Fd}, v_{x_Ld})) \quad (4)$$

where v_{x_Ld} and v_{x_Fd} are the longitudinal velocities of the vehicles L_d and F_d , respectively.

By defining the time matrix \mathbf{R} and the coefficient matrices \mathbf{P} and \mathbf{Q} , the time-dependent trajectory can be written as

$$\mathbf{R} = [1, t, t^2, t^3, t^4, t^5] \quad (5)$$

$$\mathbf{P} = [p_0, p_1, p_2, p_3, p_4, p_5]^T \quad (6)$$

$$\mathbf{Q} = [q_0, q_1, q_2, q_3, q_4, q_5]^T \quad (7)$$

$$\begin{cases} x(t) = \mathbf{R} * \mathbf{P}, v_x(t) = x'(t), a_x(t) = x''(t) \\ y(t) = \mathbf{R} * \mathbf{Q}, v_y(t) = y'(t), a_y(t) = y''(t) \end{cases} \quad (8)$$

Substituting Equations (2)–(3) into Equation (1), 10 out of 12 coefficients can be expressed as

$$\begin{cases} p_0 = q_0 = 0 \\ p_1 = v_{x0}, q_1 = 0 \\ p_2 = q_2 = 0, p_6 = \frac{6x_{lc}}{t_{lc}^5} \\ p_3 = \frac{10x_{lc}^3}{t_{lc}^3} - t_{lc}(8v_{xlc} + 12v_{x0}) \\ q_3 = \frac{10y_{lc}^3}{t_{lc}^3} - 8t_{lc}v_{ylc}, q_4 = \frac{-15y_{lc}}{t_{lc}^4} \\ p_4 = \frac{t_{lc}^4}{t_{lc}^4} + t_{lc}(14v_{xlc} + 16v_{x0}) \\ p_5 = \frac{6x_{lc}}{t_{lc}^5} - t_{lc}(6v_{xlc} + 6v_{x0}) \end{cases} \quad (9)$$

Therefore, the reference lane change trajectory S_{path} can be formulated into a function of t_{lc} and x_{lc} by defining the initial constraints as

$$S_{path} = f(t_{lc}, x_{lc}) \quad (10)$$

Since the vehicle kinematics constraints and the road regulations can also be expressed as the functions of t_{lc} and x_{lc} , the reference lane change trajectory derivation can be formulated to a constrained optimization problem by setting the cost function as a combination of indicators associated with t_{lc} and x_{lc} .

A general constrained optimization problem with both equality and inequality constraints is formulated as

$$\begin{aligned} & \min f(\xi), \xi \in R^n \\ & \text{s.t. } h_{i_linear}(\xi) = 0 \\ & h_{j_nonlinear}(\xi) = 0 \\ & g_{m_linear}(\xi) \leq 0, i, j, m, n \in Q \\ & g_{n_nonlinear}(\xi) \leq 0, i, j, m, n \in Q \end{aligned} \quad (11)$$

where ξ stands for the vector that needs to be optimized; $\mathbf{h}(\xi)$ is the linear and nonlinear equality constraints; $\mathbf{g}(\xi)$ is the linear

and nonlinear inequality constraints. This equation can be further transformed into a function with only two variables, i.e., the lane change time t_{lc} and the longitudinal displacement x_{lc} .

As the reference lane change trajectory is generated by assuming unchanged motion states of the surrounding vehicles, the collision-free-related characteristics (e.g., the distance and the relative velocity between vehicles) are excluded in the cost function. They will be accounted for in Section III and IV. Considering acceleration, jerk and road curvature, the optimization formulation is given by

$$\begin{aligned} \min J(t_f, x_f) = & w_1 \int_0^s j_{acc}^2(s) ds \\ & + w_2 \int_0^s \kappa^2(s) ds + w_3 \int_0^s acc^2(s) ds + w_4 t_f \\ \text{s.t. } & |\ddot{x}(t)|^2 \leq a_{x\max}^2 \\ & |\ddot{y}(t)|^2 \leq a_{y\max}^2 \\ & |\dot{x}(t)| \leq v_{x\max} \\ & |\dot{y}(t)| \leq v_{y\max} \\ & -\kappa_{\max} \leq \kappa(t) \leq \kappa_{\max} \end{aligned} \quad (12)$$

where ω_i ($i = 1, 2, 3, 4$) is the weighting factor; j_{acc} is the jerk to describe the rate of change of acceleration; κ is the road curvature; acc is the acceleration of the host vehicle. The curvature κ can be calculated by

$$\kappa = \frac{|x'(t)y''(t) - x''(t)y'(t)|}{[x'^2(t) + y'^2(t)]^{\frac{3}{2}}} \quad (13)$$

As the curvature in the cost function is non-convex, the sets of the lane change time t_f and the longitudinal displacement x_f are selected as

$$\begin{aligned} t_f &= \{t \mid t = t_{\min} + k_{tf} \cdot t_{\text{sample}}, k_{tf} \in N\} \\ x_f &= \{x \mid x = x_{\min} + k_{xf} \cdot x_{\text{sample}}, k_{xf} \in N\} \end{aligned} \quad (14)$$

where t_{\min} and x_{\min} are the minimal lane change time and longitudinal displacement; t_{sample} and x_{sample} are the sampling time and displacement interval.

Different lane change trajectories can be numerically acquired using t_f and x_f . A suboptimal trajectory determined by Equation (12) is treated as the initial value in the SQP derivation. If the SQP can be solved, the derived solution is used as the final optimal reference trajectory; otherwise the suboptimal trajectory will be used.

The Lagrangian multiplier method is used to solve the optimization problem. The inequality constraints are given as

$$\begin{aligned} \min f(\xi), \xi \in \mathbb{R}^n \\ \text{s.t. } g_i(\xi) \geq 0, i = 1, 2, \dots, m \end{aligned} \quad (15)$$

By introducing the auxiliary variables y_i ($i = 1, 2, \dots, m$), the equation can be formulated as

$$\begin{aligned} \min f(\xi), \xi \in \mathbb{R}^n \\ \text{s.t. } g_i(\xi) - y_i^2 = 0, i = 1, 2, \dots, m \end{aligned} \quad (16)$$

Then, the augmented Lagrangian function can be given by

$$\begin{aligned} \tilde{\psi}(\xi, y_i, \lambda, \sigma) = & f(\xi) - \sum_{i=1}^m \lambda_i [g_i(\xi) - y_i^2] \\ & + \frac{\sigma}{2} \sum_{i=1}^m [g_i(\xi) - y_i^2]^2 \end{aligned} \quad (17)$$

where λ and σ are the coefficients.

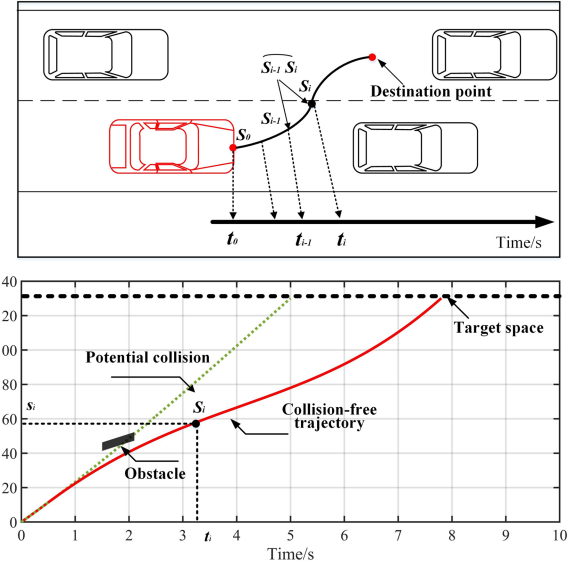


Fig. 5. Trajectories in the $X-O-Y$ coordinate system and the ST graph.

Considering the minimization respect to y_i , the auxiliary variable can be eliminated as

$$\nabla_{y_i} \tilde{\psi}(\xi, y_i, \lambda, \sigma) = 0 \quad (18)$$

The optimization termination criterion is given by

$$\sqrt{\sum_{i=1}^m \left[\min \left\{ g_i(\xi_k), \frac{(\lambda_k)_i}{\sigma} \right\} \right]^2} \leq \varepsilon \quad (19)$$

where ε is a predefined error.

III. SPEED RE-PLANNING VIA TIME SAMPLING

Abrupt acceleration changes may occur for the surrounding vehicles in real driving scenarios. A potential collision could happen if the host vehicle holds on the reference lane change trajectory. This can be avoided by the speed re-planning.

A. The ST Graph

A typical ST graph is shown in Fig. 5 [33], [34]. The horizontal axis stands for time and the vertical axis stands for arc length position along a given trajectory. The trajectory waypoints of the host vehicle are represented as a two-dimensional scale $S_i \subset \mathbb{R}^2$. The current vehicle position at a specific time step t_0 is donated as s_0 . The target position is represented as a horizontal line with a destination value s_{end} . The dynamic obstacle is expressed as the dark region as marked in Fig. 5, which indicates that the moving obstacle will overlap the trajectory in a certain time duration. In the ST domain, a potential collision can happen when the trajectory of the host vehicle overlaps the obstacle area. On the contrary, a safe and collision-free speed profile can be generated in the ST graph as long as the trajectory of the host vehicle does not cross the dark region.

B. Trajectory Cluster Generation via Speed Re-Planning

The speed at each position in the ST graph can be formulated as $v_i = f(t_i, s_i)$, where t_i and s_i are time and arc length along the

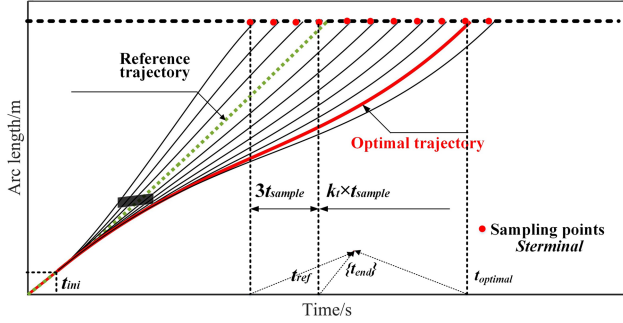


Fig. 6. Speed re-planning for collision avoidance.

trajectory. Seen from Fig. 6, the reference destination and the reference lane change time can be drawn as two lines parallel to the time and the space axis, i.e., $s = s_{\text{end}}$ and $t = t_{\text{ref}}$, respectively. By discretizing the time axis, multiple trajectory clusters can be generated by sampling the reference time state t_{ref} , in which the trajectories with collision risks or high costs would be cast away.

Define the terminal state as S_{terminal} ($s_{\text{end}}, t_{\text{end}}$), a local trajectory cluster can be obtained as the reference state, and the terminal target time sets can be derived according to the sampling step t_{sample} by

$$t_{\text{end}} = \{t | t = t_{\text{ref}} \pm k_t \cdot t_{\text{sample}}, k_t \in N\} \quad (20)$$

where $2k_t+1$ sampled trajectories can be obtained with t_{sample} denoting the time difference between the two adjacent trajectories arriving at the same destination. Hence, the terminal states of the generated trajectory cluster can be given by

$$S_{\text{terminal}} = \{(t, s) | t \in t_{\text{end}}, s = s_{\text{end}} = s_{\text{ref}}\} \quad (21)$$

where the arc length can be represented as

$$s = \int_{t_1}^{t_2} \sqrt{\left(\frac{dx}{dt}\right)^2 + \left(\frac{dy}{dt}\right)^2} dt, [t_1, t_2] \subset [0, t_{\text{end}}] \quad (22)$$

Similarly, considering that the real-time collision avoidance requires more degrees of freedom to generate a feasible trajectory from the collision-free areas in the ST graph, the quintic polynomial is used for speed re-planning. The equations of motion of the host vehicle are given by

$$s = f(t) = a_0 + b_0 t + c_0 t^2 + d_0 t^3 + e_0 t^4 + f_0 t^5 \quad (23)$$

$$v(t) = \frac{ds}{dt} \quad (24)$$

$$a(t) = \frac{d^2s}{dt^2} \quad (25)$$

Define the target variable matrix \mathbf{C} as

$$\mathbf{C} = [a_0, b_0, c_0, d_0, e_0, f_0]^T \quad (26)$$

Equations (22)-(24) can be rewritten as

$$s = \mathbf{R} \cdot \mathbf{C} \quad (27)$$

$$v = \dot{\mathbf{R}} \cdot \mathbf{C} \quad (28)$$

$$a = \ddot{\mathbf{R}} \cdot \mathbf{C} \quad (29)$$

where $\dot{\mathbf{R}} = [0, 1, 2t, 3t^2, 4t^3, 5t^4]$, $\ddot{\mathbf{R}} = [0, 0, 2, 6t, 12t^2, 20t^3]$.

The speed re-planning is essentially a process that seeks to find the optimal speed profile under the complex constraints

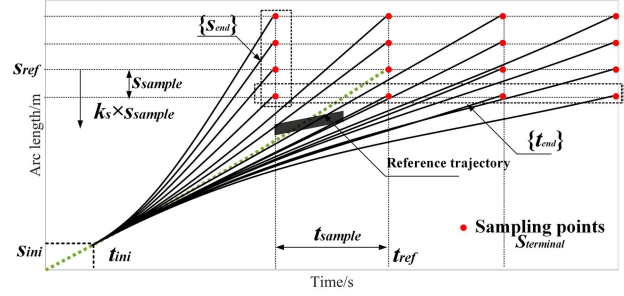


Fig. 7. Path re-planning for collision avoidance.

including the boundary state, monotonic and vehicle kinematics constraints.

1) *Boundary State Constraints:* Suppose that the speed re-planning module is triggered at the point S_{ini} ($s_{\text{ini}}, t_{\text{ini}}$), which is generated from the reference trajectory based on motion prediction and risk assessment. To guarantee that the vehicle can maintain the same initial and target states with the reference trajectory during the collision avoidance process, the constraints can be formulated as

$$s_{\text{ini}} = \mathbf{R}_{\text{ini}} \cdot \mathbf{C}_{\text{ini}} = \int_{t_0}^{t_{\text{ini}}} \sqrt{\left(\frac{dx}{dt}\right)^2 + \left(\frac{dy}{dt}\right)^2} dt \quad (30)$$

$$s_{\text{end}} = \mathbf{R}_{\text{end}} \cdot \mathbf{C}_{\text{end}} = \int_{t_0}^{t_{\text{end}}} \sqrt{\left(\frac{dx}{dt}\right)^2 + \left(\frac{dy}{dt}\right)^2} dt \quad (31)$$

where $\mathbf{C}_{\text{ini}} = \mathbf{C}_{\text{end}} = \mathbf{C}$, $\mathbf{R}_{\text{ini}} = [1, t_{\text{ini}}, t_{\text{ini}}^2, t_{\text{ini}}^3, t_{\text{ini}}^4, t_{\text{ini}}^5]$, $\mathbf{R}_{\text{end}} = [1, t_{\text{end}}, t_{\text{end}}^2, t_{\text{end}}^3, t_{\text{end}}^4, t_{\text{end}}^5]$; s_{ini} is the initial position at time step t_{ini} in the ST graph and s_{end} is the target position.

To ensure a continuous speed profile, the speeds of the collision-free cluster at S_{ini} should be expressed as

$$v_{\text{ini}} = \dot{\mathbf{R}}_{\text{ini}} \cdot \mathbf{C}_{\text{ini}} = \sqrt{\left(\frac{dx}{dt}\right|_{t_{\text{ini}}})^2 + \left(\frac{dy}{dt}\right|_{t_{\text{ini}}})^2} \quad (32)$$

where $\dot{\mathbf{R}}_{\text{ini}} = [0, 1, 2t_{\text{ini}}, 3t_{\text{ini}}^2, 4t_{\text{ini}}^3, 5t_{\text{ini}}^4]$; v_{ini} is the speed at the tangent direction at time step t_{ini} .

To increase the number of possible solutions with respect to the feasible trajectory while taking actual driving conditions into account, an interval is applied to the speed of the target waypoint, which is given by

$$v_{\text{end}} = \dot{\mathbf{R}}_{\text{end}} \cdot \mathbf{C}_{\text{end}} \in (v_{\min}, v_{\max}) \quad (33)$$

where v_{end} is the speed of the destination waypoint with $\dot{\mathbf{R}}_{\text{end}} = [0, 1, 2t_{\text{end}}, 3t_{\text{end}}^2, 4t_{\text{end}}^3, 5t_{\text{end}}^4]$; v_{\min} and v_{\max} are the variables determined by the traffic conditions, road rules and regulations. Each sampling time t_{end} corresponds to a destination speed v_{end} so that v_{end} is a set with all possible terminal states of the host vehicle satisfying

$$\left(\bigcup_{i=1}^n v_{\text{end}} \right) \subseteq (v_{\min}, v_{\max}) \quad (34)$$

where n is the number of the sampling points with $n = 2k_t+1$.

Remark 3: Considering that the acceleration of the host vehicle can change abruptly in emergency situations, the constraints of acceleration continuity are not defined separately.

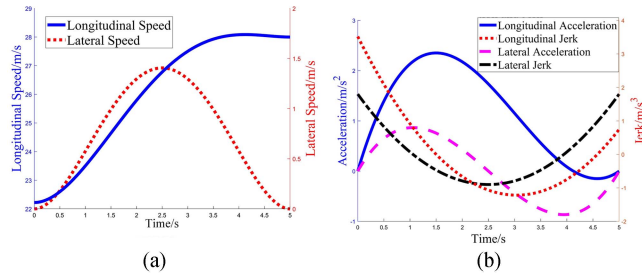


Fig. 8. (a) Speeds of the lane change trajectory. (b) Accelerations and jerks of the lane change trajectory.

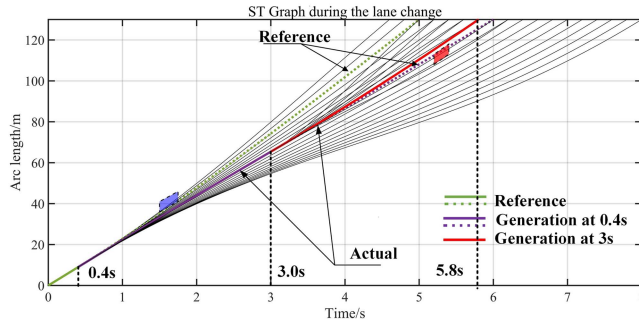


Fig. 9. Collision avoidance in the ST Graph.

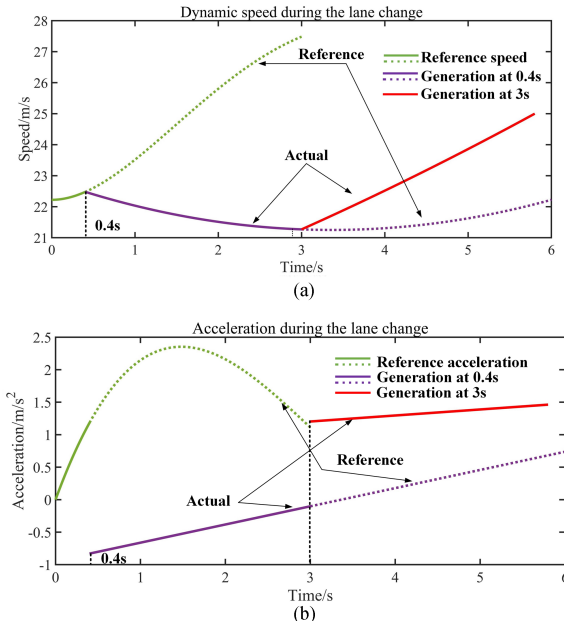


Fig. 10. (a) Speed generation during the lane change. (b) Acceleration generation during the lane change.

2) *Monotonic Constraint*: The arc length along the trajectory s with respect to time t must be monotonously increasing, so the monotonic constraint is required during trajectory optimization. By sampling m points within the time interval $[t_{ini}, t_{end}]$, the time is discretized. For the k^{th} (referring to the time stamp t_k) and $(k-1)^{th}$ (referring to the time stamp t_{k-1}) points ($k < m$), $s(t_k) > s(t_{k-1})$ must be guaranteed, which can be expressed as

$$[\mathbf{R}_{k-1} - \mathbf{R}_k] \cdot \mathbf{C} \leq 0 \quad (35)$$

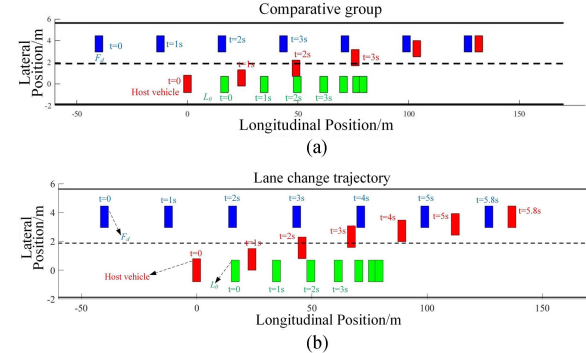


Fig. 11. (a) Without speed re-planning. (b) The proposed speed re-planning scheme.

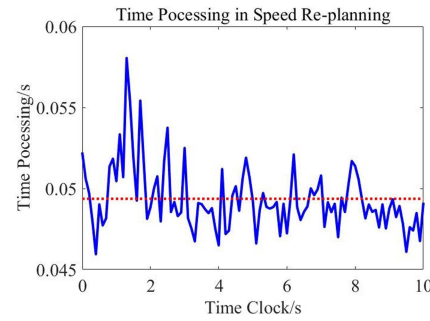


Fig. 12. Computational time of the proposed scheme.

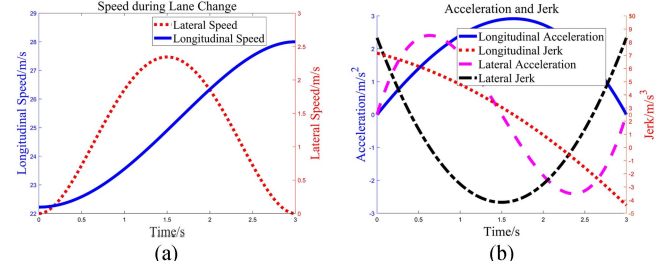


Fig. 13. (a) Speeds of the lane change trajectory. (b) Accelerations and jerks of the lane change trajectory.

where $\mathbf{R}_{k-1} = [1, t_{k-1}, t_{k-1}^2, t_{k-1}^3, t_{k-1}^4, t_{k-1}^5]$ and $\mathbf{R}_k = [1, t_k, t_k^2, t_k^3, t_k^4, t_k^5]$.

3) *Speed and Acceleration Constraints*: Considering the vehicle kinematics and actuator performance constraints, the speed and acceleration constraints with respect to the k^{th} discretized points (t_k) on the trajectory can be arranged as

$$\begin{cases} -\dot{\mathbf{R}}_k \cdot \mathbf{C} \leq -v_{min} \\ \dot{\mathbf{R}}_k \cdot \mathbf{C} \leq v_{max}, k \in [1, m] \end{cases} \quad (36)$$

where $\dot{\mathbf{R}}_k = [0, 1, 2t_k, 3t_k^2, 4t_k^3, 5t_k^4]$

$$\begin{cases} -\ddot{\mathbf{R}}_k \cdot \mathbf{C} \leq -a_{min} \\ \ddot{\mathbf{R}}_k \cdot \mathbf{C} \leq a_{max}, k \in [1, m] \end{cases} \quad (37)$$

where $\ddot{\mathbf{R}}_k = [0, 0, 2, 6t_k, 12t_k^2, 20t_k^3]$, and a_{min} and a_{max} are the accelerations related to vehicle dynamics boundaries.

Each trajectory in the trajectory cluster is an optimal solution to the target cost function with different timestamp states at t_{end} .

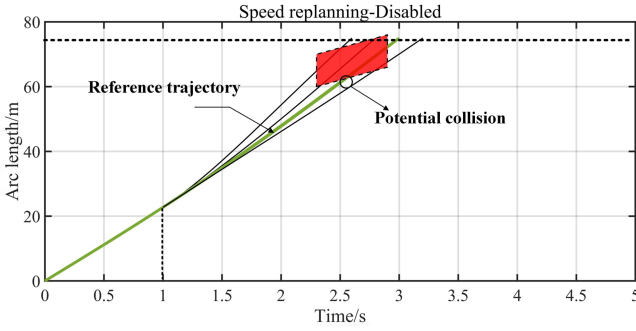


Fig. 14. No feasible trajectory solution through speed re-planning.

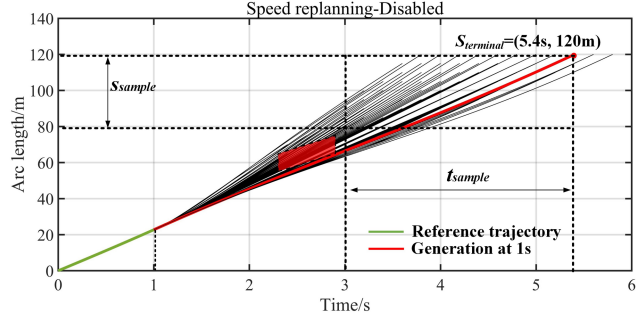


Fig. 15. Collision avoidance based on the proposed path re-planning.

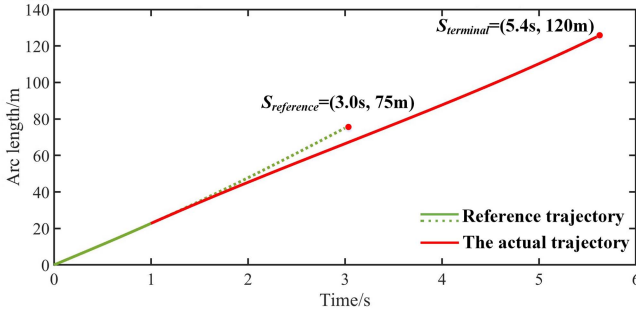


Fig. 16. Comparison of the reference and actual trajectories.

Hence, the cost function must be minimized while satisfying the constraints described above.

1) *Acceleration*: Acceleration has been widely adopted to describe ride comfort, which is given by

$$J_{acc} = \int_{t_{ini}}^{t_{end}} \ddot{f}^2(t) dt \quad (38)$$

2) *Jerk*: The term related to jerk is given by

$$J_j = \int_{t_{ini}}^{t_{end}} f'''(t) dt \quad (39)$$

The complete cost function can be expressed as

$$J_{total} = \min (w_{acc} J_{acc} + w_j J_j) \quad (40)$$

where w_{acc} and w_j are the weighting coefficients for the acceleration and the jerk term.

The above-mentioned issue can be formulated into a constrained optimization problem to obtain the optimal polynomial coefficients. Especially, the generation of the collision-free

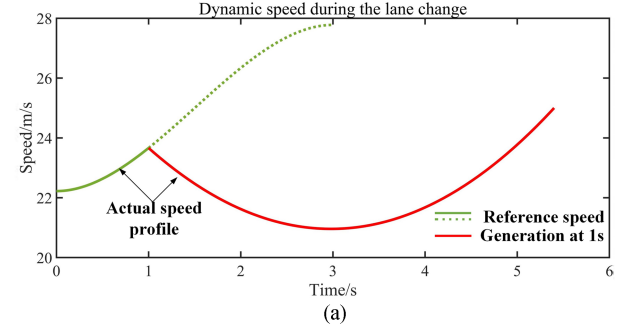


Fig. 17. (a) Speed generation during the lane change. (b) Acceleration generation during the lane change.

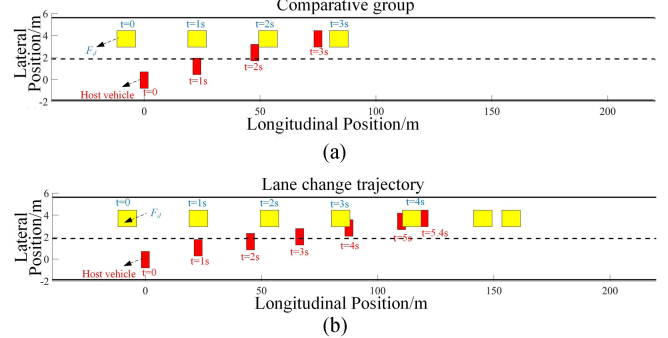


Fig. 18. (a) Without path re-planning; (b) The proposed path re-planning method.

trajectory cluster based on the speed re-planning can be transformed into a standard QP problem.

The general form of a QP problem can be given by

$$\begin{aligned} \min_{\xi \in \mathbb{R}^n} J(\xi) &= \frac{1}{2} \xi^T H \xi + f^T \xi \\ \text{s.t.} \quad a_i^T \xi &= b_i, i = 1, 2, \dots, m \\ a_i^T \xi &\geq b_i, i = m+1, \dots, p \end{aligned} \quad (41)$$

where $J(\xi)$ is the cost function, $f: \mathbb{R}^n \rightarrow \mathbb{R}$ is a function which takes a vector $\xi \in \mathbb{R}^n$ as the input and a scalar $f(\xi) \in \mathbb{R}$ as the output; H is the Hessian matrix given by

$$H = \begin{pmatrix} \frac{\partial^2 J}{\partial \xi_1^2} & \frac{\partial^2 J}{\partial \xi_1 \partial \xi_2} & \cdots & \frac{\partial^2 J}{\partial \xi_1 \partial \xi_n} \\ \frac{\partial^2 J}{\partial \xi_2 \partial \xi_1} & \frac{\partial^2 J}{\partial \xi_2^2} & \cdots & \frac{\partial^2 J}{\partial \xi_2 \partial \xi_n} \\ \vdots & \vdots & \ddots & \vdots \\ \frac{\partial^2 J}{\partial \xi_n \partial \xi_1} & \frac{\partial^2 J}{\partial \xi_n \partial \xi_2} & \cdots & \frac{\partial^2 J}{\partial \xi_n^2} \end{pmatrix} \quad (42)$$

where n is the dimension of the vector ξ .

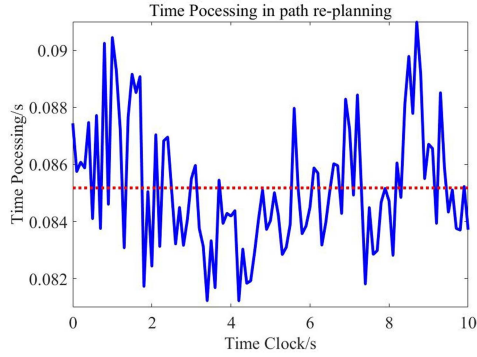


Fig. 19. Computational time of the algorithm.

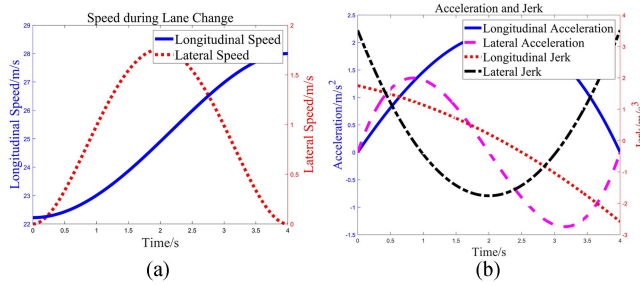


Fig. 20. (a) Speeds of the lane change trajectory. (b) Accelerations and jerks of the lane change trajectory.

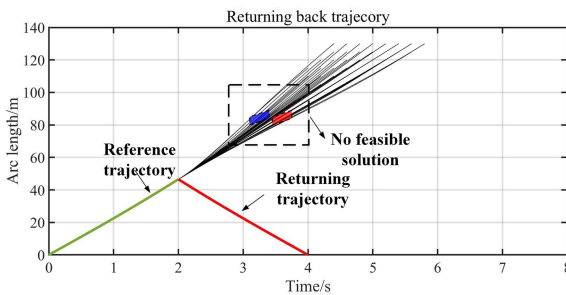


Fig. 21. No feasible trajectory solution based on the speed re-planning and the path re-planning.

If the Hessian matrix \mathbf{H} is positive definite, the QP problem is convex and the global optimal solution can be obtained by setting $\nabla \mathbf{J} = 0$. Otherwise, the cost function is often trapped into a local minimum of the non-convex function \mathbf{J} .

The cost function can be converted to a standard quadratic form by formal transformation. Substituting Equations (30)-(31) to Equations (38)-(39), the cost functions are given by

$$J_{acc} = \int_{t_{ini}}^{t_{end}} \ddot{f}^2(t) dt = \mathbf{C}^T \cdot \int_{t_{ini}}^{t_{end}} \ddot{\mathbf{R}}^T \ddot{\mathbf{R}} dt \cdot \mathbf{C} \quad (43)$$

$$J_j = \int_{t_{ini}}^{t_{end}} f^2(t) dt = \mathbf{C}^T \cdot \int_{t_{ini}}^{t_{end}} \mathbf{R}^T \mathbf{R} dt \cdot \mathbf{C} \quad (44)$$

where $\ddot{\mathbf{R}} = [0, 0, 0, 6, 24t, 60t^2]$.

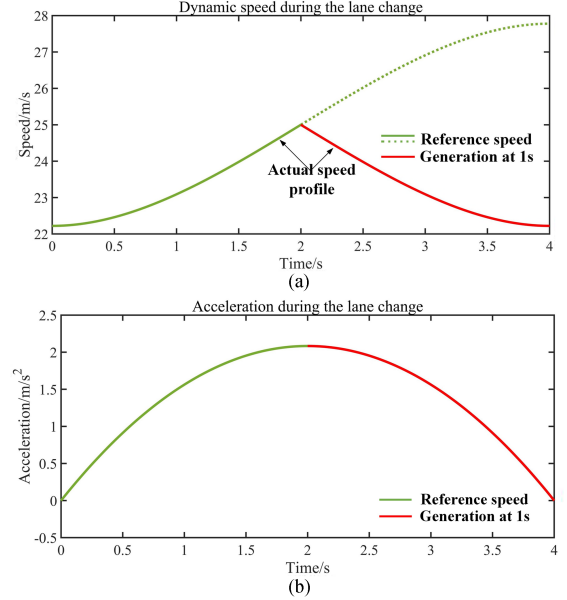


Fig. 22. (a) Speed generation during the returning process. (b) Acceleration generation during the returning process.

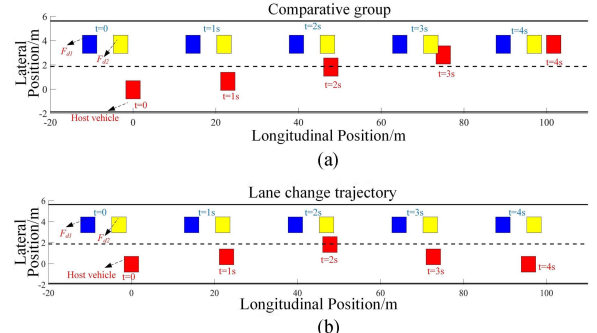


Fig. 23. (a) Without dynamic trajectory planning scheme. (b) The proposed trajectory planning scheme.

Define

$$\int_{t_{ini}}^{t_{end}} \ddot{\mathbf{R}}^T \ddot{\mathbf{R}} dt = \mathbf{H}_{acc}/2 \quad (45)$$

$$\int_{t_{ini}}^{t_{end}} \mathbf{R}^T \mathbf{R} dt = \mathbf{H}_j/2 \quad (46)$$

Then, the cost function in the standard quadratic form can be rewritten as

$$J_{acc} = \frac{1}{2} \cdot \mathbf{C}^T \cdot \mathbf{H}_{acc} \cdot \mathbf{C} \quad (47)$$

$$J_j = \frac{1}{2} \cdot \mathbf{C}^T \cdot \mathbf{H}_j \cdot \mathbf{C} \quad (48)$$

Define

$$\mathbf{H} = \begin{pmatrix} \mathbf{H}_{acc} & 0 \\ 0 & \mathbf{H}_j \end{pmatrix} \quad (49)$$

$$\boldsymbol{\xi} = [\mathbf{C}; \mathbf{C}] \quad (50)$$

The overall constrained optimization problem is formulated as

$$\begin{aligned} \min_{\xi \in \mathbb{R}^n} J_{\text{total}}(\xi) &= \frac{1}{2} \xi^T \mathbf{H} \xi + \mathbf{F}^T \xi \\ \text{s.t. } &Eqs.(32) - (37) \end{aligned} \quad (51)$$

where \mathbf{F} is a null set.

By solving the constrained optimization problem with the active set algorithm, the optimal polynomial coefficient vector x can be obtained to determine the speed profile of the collision avoidance trajectory. There may be multiple feasible collision-free trajectories generated, and this means the host vehicle can reach the destination with different time stamps without collisions. An optimal trajectory must be selected from the feasible trajectory solution cluster by considering acceleration, jerk, and driving time, which is given by

$$\min J_s = w_1 \sqrt{\frac{\int_0^s \ddot{f}^2(s) ds}{t_{\text{end}} - t_{\text{ini}}}} + w_2 \sqrt{\frac{\int_0^s \ddot{\dot{f}}^2(s) ds}{t_{\text{end}} - t_{\text{ini}}}} + w_3 t_{\text{end}} \quad (52)$$

where w_1 , w_2 and w_3 are the weighting coefficients.

IV. PATH RE-PLANNING VIA SPACE SAMPLING

The speed re-planning scheme via time sampling has been explored in Section III. However, the speed re-planning may fail to avoid potential collisions under some circumstances. Hence, the path re-planning is needed to generate a reference trajectory by sampling the target positions.

Like the speed re-planning, the host vehicle with no feasible solutions in the speed re-planning will optimize the lane change path based on the sampling method. As shown in Fig. 7, by discretizing the s and the t axis, multiple trajectory clusters can be generated via sampling the terminal state S_{terminal} . To be specific, the path re-planning module obtains a series of space state sets $\{s_{\text{end}}\}$ by sampling the space axis, and forms different terminal states with the sampled time state sets $\{t_{\text{end}}\}$ as illustrated in Section III.

Taking s_{ref} as the reference space state, the terminal target space sets can be formulated according to the space sampling step s_{sample} , which is given by

$$s_{\text{end}} = \{s | s = s_{\text{ref}} \pm k_s \cdot s_{\text{sample}}, k_s \in \mathbb{N}\} \quad (53)$$

Form the terminal vehicle state points pair S_{terminal} as

$$\begin{aligned} S_{\text{terminal}}(i, j) &= [(t_i, s_j)], i \in (1, 2k_t - 1), \\ j &\in (1, 2k_s - 1) \end{aligned} \quad (54)$$

where t_i stands for the i^{th} variable from the set t_{end} described in Equation (20) and s_j for the j^{th} variable from s_{end} .

The boundary state constraints in Equation (31) can be generated based on S_{terminal} , which can be expressed as

$$s_{\text{end}} = S_{\text{terminal}}(2) = \int_{t_0}^{S_{\text{terminal}}(1)} \sqrt{\left(\frac{dx}{dt}\right)^2 + \left(\frac{dy}{dt}\right)^2} \quad (55)$$

The monotonic constraints, speed and acceleration constraints and the cost function are similar to that in Equations (35-37) and Equation (51) presented in Section III.

Generally, by solving the constrained optimization problem, $S_{\text{terminal}}(i \times j)$ represents $(i \times j)$ trajectories based on the permutation and combination of t_{end} and s_{end} . Then, an optimal feasible trajectory can be determined by Equation (52).

During the lane change process, if the traffic flow on the target lane cannot allow the lane change maneuver, the host vehicle would be guided back onto its original lane for safety. For simplicity, the reference trajectory for returning is defined symmetrical to the first half part of the lane change maneuver. The presented collision avoidance scheme is also feasible for obstacle avoidance during the process.

V. SIMULATION VERIFICATIONS

To evaluate the performance of the proposed framework, comprehensive simulation studies are conducted in the *Matlab* software. The *fmincon* and *quadprog* software packages are used to solve the SQP and QP problems. Moreover, the ‘Real Time Sync’ module in the *Matlab/Simulink* is used to evaluate the real-time performance of the proposed scheme.

A. Case 1: Collision Avoidance via Speed Re-Planning

As shown in Fig. 1, a front vehicle L_0 on the current lane and a lag vehicle F_d on the target lane are considered. The initial speeds of the host vehicle, L_0 and F_d , are 80 km/h, 70 km/h and 100 km/h, respectively. The initial distance between L_0 and the host vehicle is set as 15 m and as 40 m between F_d and the host vehicle. The safety margin is set as 5 m. The reference lane change time and longitudinal displacement are determined as $t_{lc} = 5$ s and $x_{lc} = 130$ m based on the SQP. Fig. 8(a-b) illustrate the dynamics configurations of the lane change reference trajectory for the host vehicle.

The host vehicle will drive along the reference trajectory until potential collision risks are detected due to the unexpected accelerations of the surrounding vehicles. At the time of 0.4 s, L_0 abruptly decelerates with an acceleration of 3 m/s^2 , which is described by the purple region marked in Fig. 9. As observed, the reference trajectory may overlap with the obstacle vehicle L_0 at the time of 1.6 s. To avoid a potential collision, the host vehicle needs to sample a series of terminal states based on the reference time to generate a collision-free trajectory cluster. Owing to the reference lane change time $t_{\text{ref}} = t_{lc}$, a set of lane change time is sampled as the boundary constraints in the QP problem to check whether a feasible trajectory can be obtained.

As shown in Fig. 9, a cluster of lane change trajectories is generated at the time of 0.4 s. Then, an optimal trajectory with a longer timestamp $t_{\text{end}} = 6$ s is selected among the collision-free trajectories, which has slower speeds than the reference trajectory with $t_{\text{ref}} = 5$ s. Moreover, considering that F_d is moving at a constant speed all the time, a collision may occur due to the deceleration of the host vehicle during the first half of the lane change process. The red region marked in Fig. 9 stands for the potential collision caused by F_d , which is predicted by the host vehicle at 3.0 s. Similarly, a new cluster of trajectories starting at the specific state (3.0 s, 65.39 m) is generated by sampling a series of timestamps.

Moreover, a new terminal state (5.8 s, 130 m) considering the motion impact of F_d is determined, which denotes that the host vehicle can accelerate slightly to keep a safe distance with F_d . Hence, the host vehicle needs to adjust its speed profile twice based on collision detection. The sampling process and the feasible trajectory cluster are shown in Fig. 9. It can be seen that the host vehicle is capable of avoiding potential collisions.

by re-planning the speed profile while reaching the same destination. Moreover, the speed and acceleration profiles are given in Fig. 10(a)-(b), which show the processes of slowing down and then accelerating without violating the speed and acceleration boundary constraints. As shown in Fig. 11(a), the conventional trajectory planning method without speed re-planning is utilized to compare with the proposed algorithm. Finally, the positions of all the traffic participants with respect to time are shown in Fig. 11(b) for demonstration.

The computational efficiency of the proposed speed re-planning algorithm is verified using a laptop with an Intel Core i5-10210 CPU@1.6GHz and a 12GB RAM. The sampling interval and period are respectively selected as 0.2 s and 0.1 s, and the average processing time is 0.0483 s as shown in Fig. 12.

B. Case 2: Collision Avoidance via Path Re-Planning

A lag vehicle F_d on the target lane and the host vehicle are considered in this case. The initial speeds of F_d and of the host vehicle are 110 km/h and 80 km/h, respectively. The initial longitudinal distance between the two vehicles is set as 10 m. In order to demonstrate the effectiveness of the proposed path re-planning method, F_d is assumed to be a truck with a length of 8 m. Based on the reference trajectory derivation introduced in Section II, the reference lane change time t_{lc} and the longitudinal displacement x_{lc} are determined as 3 s and 75 m. The dynamic configurations of the lane change process are shown in Fig. 13(a-b).

The host vehicle drives along the reference trajectory until a potential collision is discerned at 1.0 s due to the high speed of F_d , and then the host vehicle attempts to avoid the collision through speed re-planning. As shown in Fig. 14, the red-marked region stands for the moving obstacle F_d , which means that F_d would cause a collision at 2.6 s if the host vehicle keeps driving along the reference trajectory. However, no feasible trajectory cluster can be obtained as F_d with a long body length has occupied all the time window. Thereby, the host vehicle resamples the spatial terminal states S_{terminal} based on the space sampling to obtain feasible collision-free trajectory clusters.

As shown in Fig. 15, through path re-planning based on $S_{\text{ref}} = (t_{\text{ref}}, s_{\text{ref}}) = (3 \text{ s}, 75 \text{ m})$, $\{t_{\text{sample}}\}$ and $\{s_{\text{sample}}\}$ are sampled to construct the feasible terminal state S_{terminal} . A series of feasible trajectories can be generated and the optimal trajectory and the terminal state (5.4 s, 120 m) are determined based on the cost function, which differs from the reference state (3 s, 75 m) on the timestamp and terminal space. As shown in Fig. 16, the host vehicle can avoid similar potential obstacles by selecting a feasible trajectory with longer time and larger displacement based on path re-planning when the speed re-planning is insufficient to tackle the situation. Moreover, the speed and acceleration profiles are given in Fig. 17(a)-(b), which illustrate the deceleration process of the host vehicle for collision avoidance. The positions of all the traffic participants are illustrated in Fig. 18(a-b). The comparison group without path re-planning could cause collision. Finally, as shown in Fig. 19, the average processing time is 0.0853 s, which also confirms the superior computational efficiency of the speed re-planning over the path re-planning.

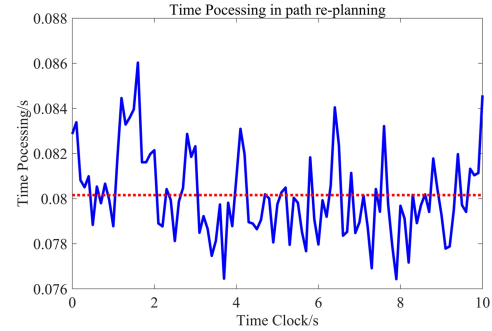


Fig. 24. Computational time of the algorithm.

C. Case 3: Returning to the Original Lane

Two lag vehicles F_{d1} and F_{d2} on the target lane and the host vehicle are considered in this case. The dynamic configurations of the lane change process are shown in Fig. 20(a)-(b) with a reference state $S_{\text{reference}} = (4 \text{ s}, 100 \text{ m})$. At 2.0 s, it is predicted that the spatial sampling with respect to both space and time is occupied by the two obstacle vehicles (see Fig. 21). To avoid potential collisions, the host vehicle will be guided back onto its original lane. For calculation simplification, the trajectory back to the origin lane is set to be symmetric with the first half lane change trajectory as shown in Fig. 22(a)-(b). Finally, the positions of all the vehicles during the returning process of the comparison group (without dynamic trajectory planning) and of the proposed collision avoidance scheme are given in Fig. 23(a-b). The average processing time for this case is 0.0801 s as shown in Fig. 24. The hierarchical collision avoidance algorithm is also applicable to the collision avoidance when driving back onto the original lane.

VI. CONCLUSION

In this paper, a hierarchical lane change framework is proposed to realize real-time obstacle avoidance while improving safety, comfort and traffic efficiency of the transport. A quintic polynomial lane change reference trajectory is obtained via the Sequential Quadratic Programming (SQP) by assuming unchanged motion states of the surrounding vehicles. In practical driving scenarios, the speed re-planning module will be executed if a potential collision risk is discerned. The QP-based collision-free trajectory cluster can be generated through time sampling. If no feasible trajectories can be extracted from the speed re-planning, the vehicle will sample both time and space to seek for new collision-free trajectory clusters. The optimal lane change trajectory is determined by a cost function considering acceleration, jerk and traffic efficiency. If all the two modules fail to obtain a feasible solution, the vehicle will be guided back onto its original lane. The effectiveness of the proposed scheme is verified under three typical traffic scenarios.

REFERENCES

- [1] J. Rios-Torres and A. A. Malikopoulos, "A survey on the coordination of connected and automated vehicles at intersections and merging at highway on-ramps," *IEEE Trans. Intell. Transp. Syst.*, vol. 18, no. 5, pp. 1066–1077, May 2017.

- [2] L. Zhang *et al.*, "Chassis coordinated control for full X-by-Wire Vehicles-A review," *Chin. J. Mech. Eng.*, vol. 34, no. 1, pp. 1–25, 2021.
- [3] B. Paden, M. Cap, S. Z. Yong, D. Yershov, and E. Frazzoli, "A survey of motion planning and control techniques for self-driving urban vehicles," *IEEE Trans. Intell. Veh.*, vol. 1, no. 1, pp. 33–55, Mar. 2016.
- [4] M. Schmidt, C. Manna, J. H. Braun, C. Wissing, M. Mohamed, and T. Bertram, "An interaction-aware lane change behavior planner for automated vehicles on highways based on polygon clipping," *IEEE Robot. Automat. Lett.*, vol. 4, no. 2, pp. 1876–1883, Apr. 2019.
- [5] F. You *et al.*, "Trajectory planning and tracking control for autonomous lane change maneuver based on the cooperative vehicle infrastructure system," *Expert Syst. Appl.*, vol. 42, no. 14, pp. 5932–5946, 2015.
- [6] S. Yim, "Preview controller design for vehicle stability with V2V communication," *IEEE Trans. Intell. Transp. Syst.*, vol. 18, no. 6, pp. 1497–1506, Jun. 2017.
- [7] C. Hubmann, J. Schulz, M. Becker, D. Althoff, and C. Stiller, "Automated driving in uncertain environments: Planning with interaction and uncertain maneuver prediction," *IEEE Trans. Intell. Veh.*, vol. 3, no. 1, pp. 5–17, Mar. 2018.
- [8] D. Gonzalez, J. Perez, V. Milanes, and F. Nashashibi, "A review of motion planning techniques for automated vehicles," *IEEE Trans. Intell. Transp. Syst.*, vol. 17, no. 4, pp. 1135–1145, Apr. 2016.
- [9] L. Zhang, Z. Wang, X. Ding, S. Li, and Z. Wang, "Fault-Tolerant control for intelligent electrified vehicles against front wheel steering angle sensor faults during trajectory tracking," *IEEE Access*, vol. 9, pp. 65174–65186, 2021.
- [10] Y. Huang *et al.*, "A motion planning and tracking framework for autonomous vehicles based on artificial potential field elaborated resistance network approach," *IEEE Trans. Ind. Electron.*, vol. 67, no. 2, pp. 1376–1386, Feb. 2020.
- [11] B. Okumura *et al.*, "Challenges in perception and decision making for intelligent automotive vehicles: A case study," *IEEE Trans. Intell. Veh.*, vol. 1, no. 1, pp. 20–32, Mar. 2016.
- [12] B. Paden, M. Cáp, S. Z. Yong, D. Yershov, and E. Frazzoli, "A survey of motion planning and control techniques for self-driving urban vehicles," *IEEE Trans. Intell. Veh.*, vol. 1, no. 1, pp. 33–55, Apr. 2016.
- [13] L. Chen *et al.*, "A path and velocity planning method for lane changing collision avoidance of intelligent vehicle based on cubic 3-D Bezier curve," *Adv. Eng. Softw.*, vol. 132, pp. 65–73, 2019.
- [14] X. Hu *et al.*, "Dynamic path planning for autonomous driving on various roads with avoidance of static and moving obstacles," *Mech. Syst. Signal Process.*, vol. 100, pp. 482–500, 2018.
- [15] M. Yue, X. Hou, X. Zhao, and X. Wu, "Robust tube-based model predictive control for lane change maneuver of tractor-trailer vehicles based on a polynomial trajectory," *IEEE Trans. Syst., Man, Cybern., Syst.*, vol. 50, no. 12, pp. 5180–5188, Dec. 2020.
- [16] J. Zhou, H. Zheng, J. Wang, Y. Wang, B. Zhang, and Q. Shao, "Multiobjective optimization of lane-changing strategy for intelligent vehicles in complex driving environments," *IEEE Trans. Veh. Technol.*, vol. 69, no. 2, pp. 1291–1308, Feb. 2020.
- [17] R. Cui, Y. Li, and W. Yan, "Mutual information-based Multi-AUV path planning for scalar field sampling using multidimensional RRT*," *IEEE Trans. Syst., Man, Cybern., Syst.*, vol. 46, no. 7, pp. 993–1004, Jul. 2016.
- [18] D. Devaurs, T. Simeon, and J. Cortes, "Optimal path planning in complex cost spaces with sampling-based algorithms," *IEEE Trans. Automat. Sci. Eng.*, vol. 13, no. 2, pp. 415–424, Apr. 2016.
- [19] Y. Rasekipour, A. Khajepour, S.-K. Chen, and B. Litkouhi, "A potential field-based model predictive path-planning controller for autonomous road vehicles," *IEEE Trans. Intell. Transp. Syst.*, vol. 18, no. 5, pp. 1255–1267, May 2017.
- [20] B. Zhu, S. Yan, J. Zhao, and W. Deng, "Personalized lane-change assistance system with driver behavior identification," *IEEE Trans. Veh. Technol.*, vol. 67, no. 11, pp. 10293–10306, Nov. 2018.
- [21] T. Peng *et al.*, "A new safe lane-change trajectory model and collision avoidance control method for automatic driving vehicles," *Expert Syst. Appl.*, vol. 141, 2020, Art. no. 112953.
- [22] D. Zeng *et al.*, "A novel robust lane change trajectory planning method for autonomous vehicle," in *Proc. IEEE Intell. Veh. Symp.*, 2019, pp. 486–493.
- [23] Y. Chen, Y. Cai, J. Zheng, and D. Thalmann, "Accurate and efficient approximation of clothoids using Bézier curves for path planning," *IEEE Trans. Robot.*, vol. 33, no. 5, pp. 1242–1247, Oct. 2017.
- [24] Q. Wang, Z. Li, and L. Li, "Investigation of discretionary lane-change characteristics using next-generation simulation data sets," *J. Intell. Transp. Syst.*, vol. 18, no. 3, pp. 246–253, 2014.
- [25] J. Ji, A. Khajepour, W. W. Melek, and Y. Huang, "Path planning and tracking for vehicle collision avoidance based on model predictive control with multiconstraints," *IEEE Trans. Veh. Technol.*, vol. 66, no. 2, pp. 952–964, Feb. 2017.
- [26] Y. Luo *et al.*, "A dynamic automated lane change maneuver based on vehicle-to-vehicle communication," *Transp. Res. Part C, Emerg. Technol.*, vol. 62, pp. 87–102, 2016.
- [27] D. Yang *et al.*, "A dynamic lane-changing trajectory planning model for automated vehicles," *Transp. Res. Part C, Emerg. Technol.*, vol. 95, pp. 228–247, 2018.
- [28] P. Cao *et al.*, "Analysing driving efficiency of mandatory lane change decision for autonomous vehicles," *IET Intell. Transport Syst.*, vol. 13, no. 3, pp. 506–514, 2019.
- [29] J. Dahl, G. R. de Campos, C. Olsson, and J. Fredriksson, "Collision avoidance: A literature review on threat-assessment techniques," *IEEE Trans. Intell. Veh.*, vol. 4, no. 1, pp. 101–113, Feb. 2019.
- [30] M. Bahram, C. Hubmann, A. Lawitzky, M. Aeberhard, and D. Wollherr, "A combined Model- and Learning-Based framework for interaction-aware maneuver prediction," *IEEE Trans. Intell. Transp. Syst.*, vol. 17, no. 6, pp. 1538–1550, Jun. 2016.
- [31] Y. Zhang, J. Li, Y. Guo, C. Xu, J. Bao, and Y. Song, "Vehicle driving behavior recognition based on multi-view convolutional neural network with joint data augmentation," *IEEE Trans. Veh. Technol.*, vol. 68, no. 5, pp. 4223–4234, May 2019.
- [32] H. Xie *et al.*, "A hybrid method combining Markov prediction and fuzzy classification for driving condition recognition," *IEEE Trans. Veh. Technol.*, vol. 67, no. 11, pp. 10411–10424, Nov. 2018.
- [33] W. Lim, S. Lee, M. Sunwoo, and K. Jo, "Hierarchical trajectory planning of an autonomous car based on the integration of a sampling and an optimization method," *IEEE Trans. Intell. Transp. Syst.*, vol. 19, no. 2, pp. 613–626, Feb. 2018.
- [34] M. Wang, Z. Wang, L. Zhang, and D. G. Dorrell, "Speed planning for autonomous driving in dynamic urban driving scenarios," in *Proc. IEEE Energy Convers. Congr. Expo.*, 2020, pp. 1462–1468.



Zhiqiang Zhang is currently working toward the Ph.D. degree in mechanical engineering with the School of Mechanical Engineering, Beijing Institute of Technology, Beijing, China. His research interests include vehicle dynamics and active safety control for intelligent electric vehicles.



Lei Zhang (Member, IEEE) received the Ph.D. degree in mechanical engineering from the Beijing Institute of Technology, Beijing, China, in 2016, and the Ph.D. degree in electrical engineering from the University of Technology, Sydney, Australia, in 2016. He is currently an Associate Professor with the School of Mechanical Engineering, Beijing Institute of Technology. His research interests include the area of control theory and engineering applied to electrified vehicles with emphases on battery management techniques, vehicle dynamics control and autonomous

driving technology. Dr. Zhang is a Member of China Society of Automotive Engineers (CSAE). He is the Technical Committee on Vehicle Control and Intelligence and the Technical Committee on Parallel Intelligence in the Chinese Association of Automation (CAA). He was the Guest Editors of several journals, including the *International Journal of Vehicle Design*, *Chinese Journal of Mechanical Engineering*, and *China Journal of Highway and Transport*. He is an Associate Editor for *Proceedings of the Institution Of Mechanical Engineers Part C-Journal Of Mechanical Engineering Science*, *SAE International Journal Of Connected And Autonomous Vehicles*, and *SAE Journal Of Electrified Vehicles*. He is also on the Editorial Boards of *Electronics*, *Sustainability* and *China Journal Of Highway And Transport*.



Junjun Deng born in 1985, is currently an Associate Professor with the School of Mechanical Engineering, Beijing Institute of Technology, Beijing, China.



Mingqiang Wang born in 1993, is currently working toward the Ph.D. degree in mechanical engineering with the National Engineering Laboratory for Electric Vehicles, Beijing Institute of Technology, Beijing, China. His research interests mainly include motion trajectory planning, trajectory tracking, and safety control for electric vehicles.



Dongpu Cao (Member, IEEE) received the Ph.D. degree from Concordia University, Canada, in 2008. He is the Canada Research Chair in Driver Cognition and Automated Driving, and currently an Associate Professor and the Director of Waterloo Cognitive Autonomous Driving (CogDrive) Lab with the University of Waterloo, Canada. His current research interests include driver cognition, automated driving and cognitive autonomous driving. He has contributed more than 200 papers and three books. He was the recipient of the SAE Arch T. Colwell Merit Award in 2012, IEEE VTS 2020 Best Vehicular Electronics Paper Award and three best paper awards from the ASME and IEEE conferences. Prof. Cao is the Deputy Editor-in-Chief for IET *Intelligent Transport Systems Journal*, and an Associate Editor for IEEE TRANSACTIONS ON VEHICULAR TECHNOLOGY, IEEE TRANSACTIONS ON INTELLIGENT TRANSPORTATION SYSTEMS, IEEE/ASME TRANSACTIONS ON MECHATRONICS, IEEE TRANSACTIONS ON INDUSTRIAL ELECTRONICS, IEEE/CAA JOURNAL OF AUTOMATICA SINICA, IEEE TRANSACTIONS ON COMPUTATIONAL SOCIAL SYSTEMS, and ASME *Journal of Dynamic Systems, Measurement and Control*. He was the Guest Editor of *Vehicle System Dynamics*, IEEE TRANSACTIONS ON SMC: SYSTEMS AND IEEE INTERNET OF THINGS JOURNAL. He is the SAE Vehicle Dynamics Standards Committee and acts as the Co-Chair of IEEE ITSS Technical Committee on Cooperative Driving. Prof. Cao is an IEEE VTS Distinguished Lecturer.



Zhenpo Wang (Member, IEEE) born in 1976, received the Ph.D. degree in automotive engineering from the Beijing Institute of Technology, Beijing, China, in 2005. He is currently a Professor with the School of Mechanical Engineering, Beijing Institute of Technology, Beijing, China.